Laser Profiling: A Promising Technique To Accurately Assess Pipe State And Roughness

Mathieu Lepot[1], Nikola Stanić[1], François H. L. R. Clemens[1,2], Mélanie Catieau[1] and Bart H. G. Goes

[1]Department of Watermanagement, Faculty of Civil Engineering and Geoscience, Technical University of Delft, Stevinweg 1 (Building 23), 2628CN Delft, The Netherlands (Email: *m.j.lepot@tudelft.nl*)
[2]Deltares, PO Box 177, 2600 MH Delft, The Netherlands (Email: *francois.clemens@deltares.nl*)

Abstract
Sewer managers aim at identifying the required information on the structural and hydraulic performance of sewer pipes in order to achieve the efficiency gains for urban drainage system management. To successfully achieve this, managers need accurate and robust data to accurately estimate the actual state of individual objects and the system as a whole. For that purpose, various techniques can be implemented (e.g. visual inspection, laser profiling). A first prototype of a laser profiler was developed to improve the accuracy of collected data. However, there is a need of more accurate apparatus. The new design presented here provides accurate measurements of the cross section and, from frame to frame, an accurate 3D image of a pipe. The potential applications of the improved laser profiling technique are comprehensive e.g. replacement of inaccurate visual inspection, deposit measurements, roughness measurements.

Keywords
Laser inspection, uncertainties, hydraulic capacities, deposits, sewers, assessment.

INTRODUCTION

Urban drainage systems as part of underground linear infrastructures are capital-intensive and have an anticipated long service life. With aging these infrastructures require more and more maintenance and managers have to minimise their maintenance costs, while being urged to keep the risk of failures and disruption at an acceptable level. Therefore, the current status of object constituting a sewer system and their evolution of deterioration need to be studied appropriately. Wirahadikusumah *et al*. (1998) present an overview of a several techniques available for sewer pipe inspections: visual inspection by closed circuit television (CCTV), radar, acoustic techniques, sonar, laser profiling or a combination of these technologies in order to benefit from the strengths of each technology. The most commonly used technique (CCTV) is relatively subjective and limited to defects that can be detected visually (Dirksen *et al.*, 2013): there is a lack of suitable information on the status of the sewer for adequate asset management. Laser profiling techniques were used for over a decade: *i*) to detect and try to quantify significant deformations or structural damages, *ii*) to quantify wall loss due to corrosion (Kirkham *et al.*, 2000). Most of previous laser profiling technique studies are biased: the position and orientation of the profiler were not taken into account. This error leads to over-estimation of wall losses and may lead to repair or replacement of reaches that still fit functional requirements. Clemens *et al.* (2014) propose an unbiased prototype for sewer inspections. This present study describes a second version of this profiler (more accurate and less bias – calibration and distortion), by increasing the camera resolutions and accuracies of laser distance meters. Detailed information on hardware and data acquisition software are published under the common creative license CC BY-NC-SA (https://creativecommons.org/licenses/by-nc-sa/3.0/). A website (http://www.sanitaryengineering.tudelft.nl/sewerinspections) devoted to sewer

inspections was recently uploaded to share all the required information, tutorials and data acquisition software for processing of the raw data.

MATERIALS AND METHODS

Materials: the laser profiler

The prototype is divided in two parts: *i*) a fixed one where laser distance meters have been set up in order to know and correct the position of the *ii*) a moving one with the laser profiler itself. In order to avoid cable length limitation or unexpected misconnection due to friction, there is no wire connection between both parts. The Figure 1 provides a graphical overview of the system.

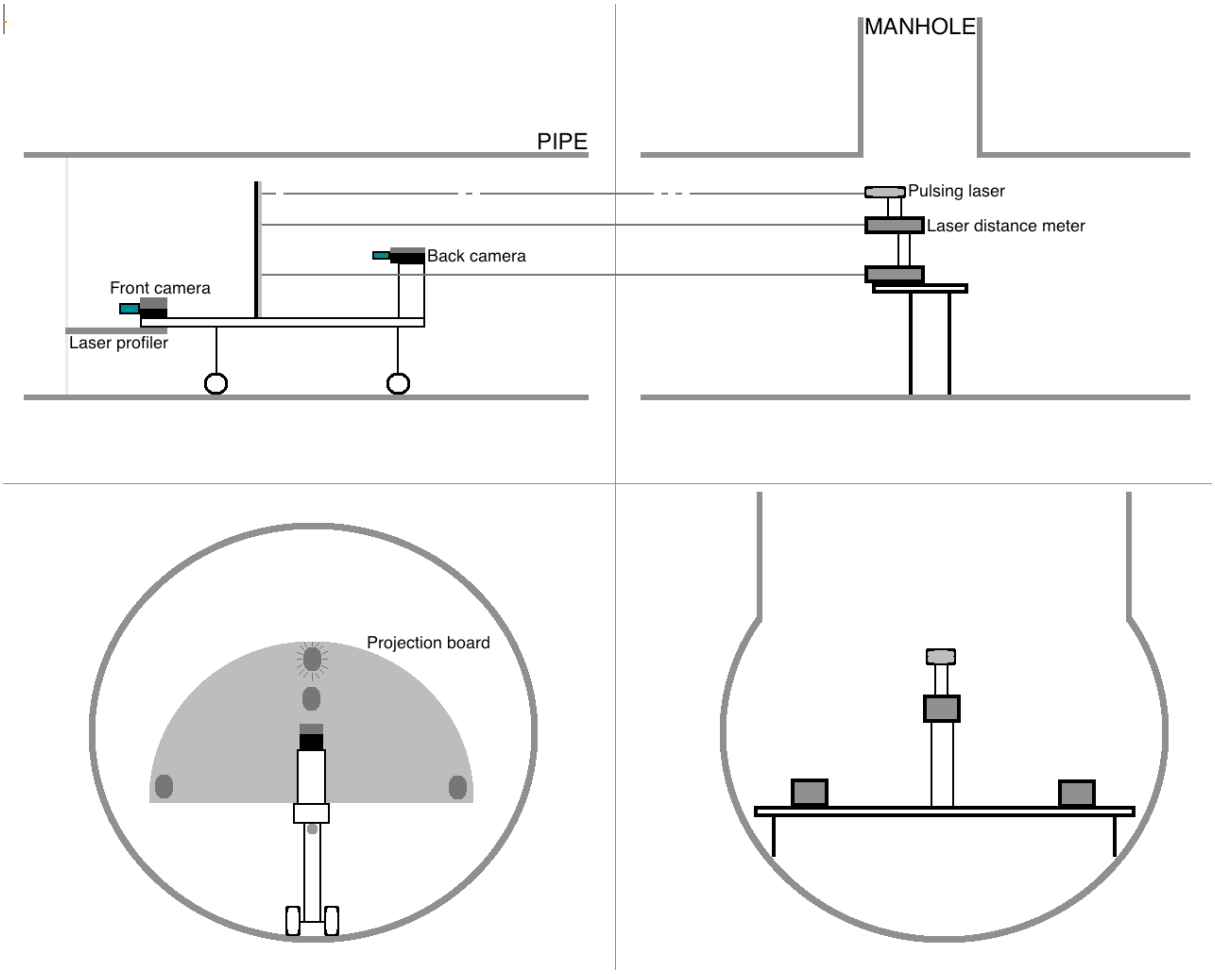

Figure 1. Schemes of the fixed (right) and the moving (left) part of this laser profiler: side (top) and back (bottom) views.

Fixed part. The fixed platform of the set-up consists of three laser distance meters (Dimetix, FLS-C10) each measuring the distance between the fixed part and a reflective board placed on the moving part. In order to ensure synchronization between both part (see details hereafter), a pulsing laser (Osela, Streamline laser (660 nm)) was also installed. The relative positions of the three lasers distance meters were optimized by a program written in Matlab® to reduce uncertainties according to a given set of sewer dimensions, accuracy in distance metering and geometrical properties. The laser distance meters were connected to a laptop through a converter RS232-USB (National Instrument, USB-232/4) and the pulsing laser were controlled by the USB Chassis (National

Instrument, cDAQ-9171) and the card (National Instrument, NI 9472). One battery of 11.1V (Robbe, Roxxy® 3S/5000 mAh) was used as power supply for the fixed part sensors.

Moving part. On the moving part, the following devices was mounted: a laser profiler (Ibak - ILP) combined with a camera (Allied Vision Technology, Prosilica GT3400C), referred to as cam_{FRONT}. The laser profiler uses a reflecting cone to project a laser sheet on the inner pipe wall, creating a line perpendicular to the profiler and thus the moving platform of the apparatus which is captured by the cam_{FRONT} (Allied Vision Technology, Manta G-282C). Three different lenses were tested and can be chosen according to their accuracies and the geometry of the pipe to inspect (Kowa, LM3NCM, LM4NCM and LM6HC). All these materials were mounted on a CCTV tractor. Due to the amount of data, a high powerful computer (Apple, Mac Pro 2013) has been used for image acquisition. Two batteries of 22.2V (Pichler, Lemon RC 6S/4400 mAh) provide energy supply the cameras.

Synchronization between both parts. Because two different computers recorded the data, with different clocks (with an unknown and non-constant lag between both clocks), a synchronization tool was required. This was ensured with a 4th laser, behaving like a pulse laser through a bijective time series On-Off on the fixed platform, the projected dots on the moving part were recorded by the back camera. In this manner the computer clocks were synchronized, at the speed of light, with this wireless solution.

Methods: Calibration, correction and data treatment

The Figure 2 presents a quick overview of the different steps required to process the data from raw measurements until the corrected and unbiased 3d image of the pipe.

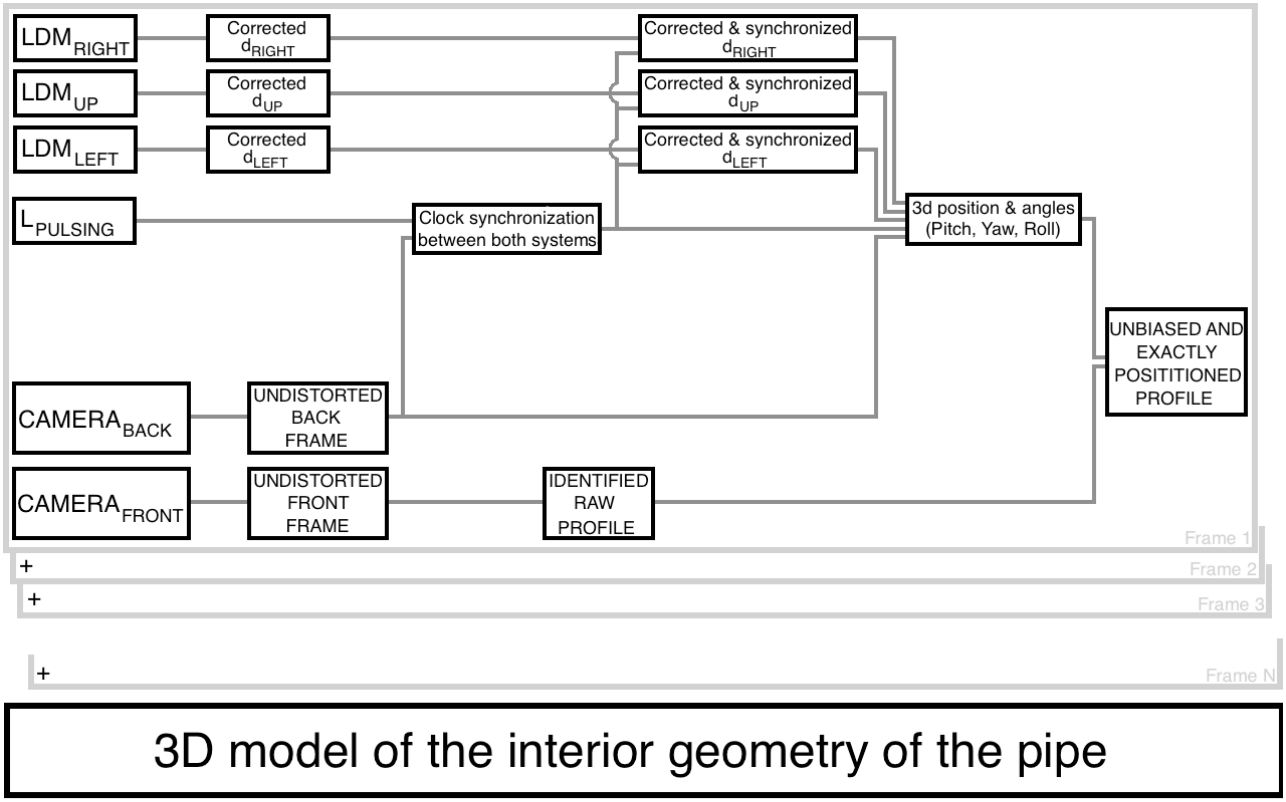

Figure 2. Principal steps of the data treatment.

Some steps (camera and laser distance meter calibration, laser misalignments and data treatment) are briefly described hereafter. Additional details have been given in Clemens *et al*. (2014) and on the website previously cited.

Camera calibration. Cameras and lenses create distortionin the recorded images due the construction of the lenses and optical refractions. In order to know the true position of lasers (recorded by both cameras), distortion corrections have to be applied. For each of the six camera-lens combinations and for each aperture of the lenses, distortion calibration was performed by the Matlab® Single Camera Calibration App, based on Heikkila and Silvèn (1997) and with 100 images per settings in order to asset uncertainties and distributions of the five distortion coefficients (Equations 1). Nine different positions of a checkerboard pattern (chessboard square size of 40 mm) were recorded: -15, 0 and +15 degrees for rotation angles for the vertical and the horizontal axes. Vignetting and respectively chromatic aberrations have been neglected due to independency of the method of these optical effects.

$$\begin{cases} x_{distored} = x \cdot (1 + k_1 \cdot r^2 + k_2 \cdot r^4 + k_3 \cdot r^6) \\ y_{distored} = y \cdot (1 + k_1 \cdot r^2 + k_2 \cdot r^4 + k_3 \cdot r^6) \\ x_{distored} = x + \left[2 \cdot p_1 \cdot y + p_2 \cdot (r^2 + 2 \cdot x^2)\right] \\ y_{distored} = y + \left[2 \cdot p_2 \cdot x + p_1 \cdot (r^2 + 2 \cdot y^2)\right] \end{cases} \quad (1)$$

Where x and y are undistorted pixel locations, $x_{distorted}$ and $y_{distorted}$ are distorted pixel locations, $r^2 = x^2 + y^2$, k_1, k_2 and k_3 are the radial distortion coefficients of the lens and p_1 and p_2 are the tangential ones. Median values of those coefficients are given in Table 1.

Table 1. The camera-lens-aperture the camera calibrations median values.

Camera	Lens	Aperture	k_1	k_2	k_3	p_1	p_2	Skew	Mean error in pixels
cam_{FRONT}	Kowa (LM4NCM)	1.6	-0.07	0.08	-0.04	-0.00	0.00	-0.83	0.44
		16	-0.08	0.12	-0.07	0.00	0.00	-0.94	0.45
	Kowa (LM3NCM)	2.4	-0.05	0.09	-0.04	0.00	0.00	-0.81	0.54
		4	-0.06	0.09	-0.04	0.00	0.00	-0.64	0.51
		8	-0.06	0.09	-0.04	0.00	0.00	-0.67	0.50
	Kowa (LM6HC)	1.8	-0.17	0.12	-0.03	0.00	0.00	-1.12	0.55
		2.8	-0.17	0.11	-0.02	0.00	0.00	-1.42	0.55
		4	-0.17	0.11	-0.03	0.00	0.00	-1.46	0.55
		5.6	-0.17	0.11	-0.03	0.00	0.00	-1.42	0.56
		8	-0.17	0.12	-0.03	0.00	0.00	-1.40	0.58
		11	-0.17	0.11	-0.03	0.00	0.00	-1.35	0.56
cam_{BACK}	Kowa (LM4NCM)	1.6	-0.08	0.10	-0.06	0.00	0.00	-1.40	0.44
		16	-0.08	0.11	-0.07	0.00	0.00	-1.08	0.51
	Kowa (LM3NCM)	2.4	-0.05	0.07	-0.03	0.00	0.00	-1.11	0.77
		4	-0.06	0.09	-0.04	0.00	0.00	-1.22	0.58
		8	-0.06	0.09	-0.04	0.00	0.00	-1.20	0.52

	1.8	-0.18	0.17	-0.09	-0.00	0.00	-0.73	0.39
	2.8	-0.18	0.16	-0.08	-0.00	0.00	-0.84	0.40
Kowa	4	-0.18	0.17	-0.08	-0.00	0.00	-0.82	0.39
(LM6HC)	5.6	-0.18	0.17	-0.08	-0.00	0.00	-0.82	0.40
	8	-0.18	0.16	-0.06	-0.00	0.00	-0.95	0.43
	11	-0.18	0.18	-0.10	-0.00	0.00	-0.90	0.44

Laser distance meter calibration. The three laser distance meters were calibrated using the ordinary least squares method on a flowmeter calibration flume and for distances varying from 1 to 30 m. Monte-Carlo simulations were used to estimate the regression coefficients, their standard uncertainties and covariance between them, in a similar way as described in Bertrand-Krajewski (2008). Due the linearity of the calibration function (Figure 3), only straight lines were calculated. From measurement uncertainties (Dimetix, 2012) and the calibration data, corrected distances and their uncertainties were calculated.

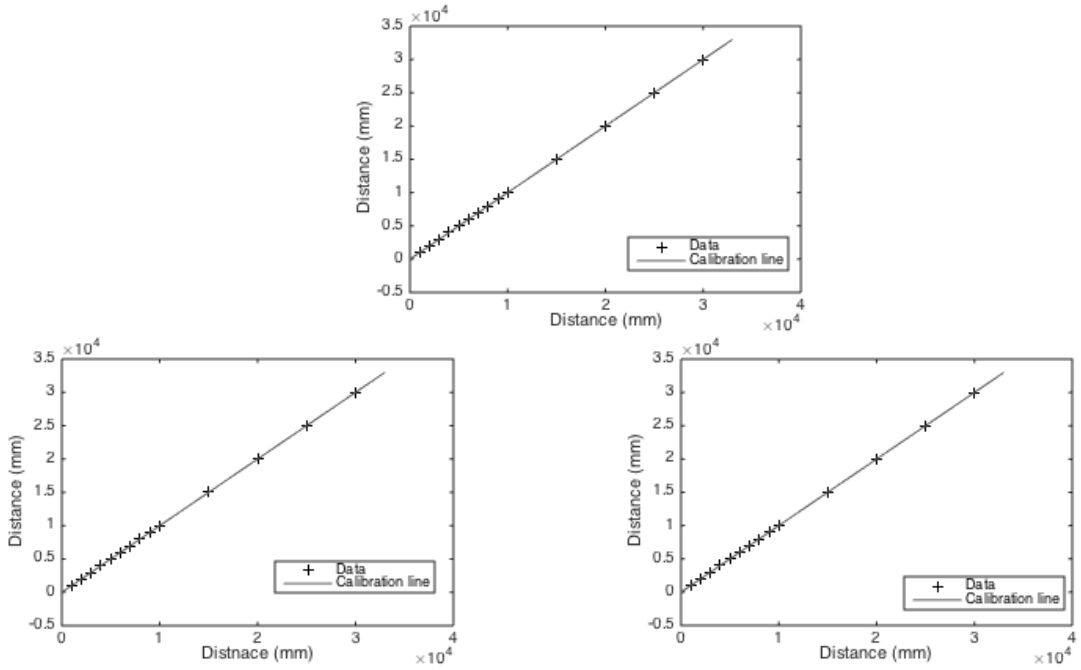

Figure 3. Calibration straight lines of the laser distance meters (top, top laser), bottom (left and right laser according to the position of Figure 1).

Laser alignment. Due to construction processes, the three laser distance meters of the fixed part are not exactly parallel. Further calculations require perfectly aligned lasers. The alignment of the lasers has been manually ensured along a 10 m distance: the lasers have been installed on a fixed controlled carriage at one side and a flat PVC board (where the laser distance projection points were carved in) perfectly perpendicular to the pipe axes has been installed on the other side. The positions of the lasers have been manually adjusted until the moment when all the laser distances were equal and the projections were positioned in the centre of printed points.

Data processing. Processing of raw data is presented in Figure 2. All the details about the methods and the mathematics applied in the data processing were addressed and published in Clemens *et al*.

(2014). The method presents the calculation until the construction of the 3D image of pipes and its uncertainties. Subsequent steps to calculate parameters or characteristics of a pipe are described in second paper devoted to application examples (*e.g.* of roughness assessment in Stanić *et al.* (2015)).

RESULTS AND DISCUSSION

The first experiments were conducted on one sewer pipe using the 1st (old) version of the laser profiling device (see Clemens *et al.* (2014)) followed by the application of the 2nd (new) version on the same pipe in order to compare the two versions. Figure 4 presents a comparative measurement between the two versions of the device.

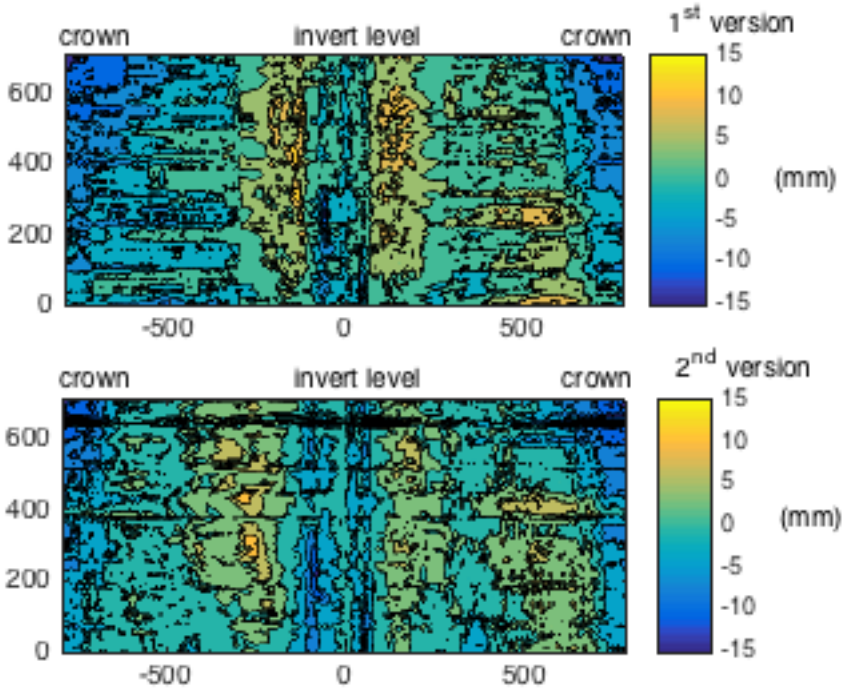

Figure 4. Difference between theoretical and measured geometries on an used 400/600 mm egg-shaped concrete pipe (top: old version, bottom: new version).

The results show that there is a difference in estimation of the loss of wall thickness, due to the fact that the distortion of the image and consequently its corrections were not taken into account within the 1st version of the prototype. This figure highlights that the correction of camera distortion is mandatory for such technique.

Uncertainty analysis was performed to determine the standard uncertainties in the x, y (section) and z (along the reach) directions. Assuming that the uncertainties in the x and y directions are mutually independent, the uncertainty of each points of the internal pipe section has been determined. The Figure 5 shows the standard uncertainties of loss of wall thickness for both prototype versions. The results show the improvements added by the new hardware and improved protocols applied. From the figure it can be seen that the standard uncertainties vary from 1 to 1.8 mm for the 2nd (new) version of the device. While for the 1st (old) version of the device, the standard uncertainty varies from 4.5 to 11.5 mm: the new design increases the accuracy with a factor of 5 to 10.

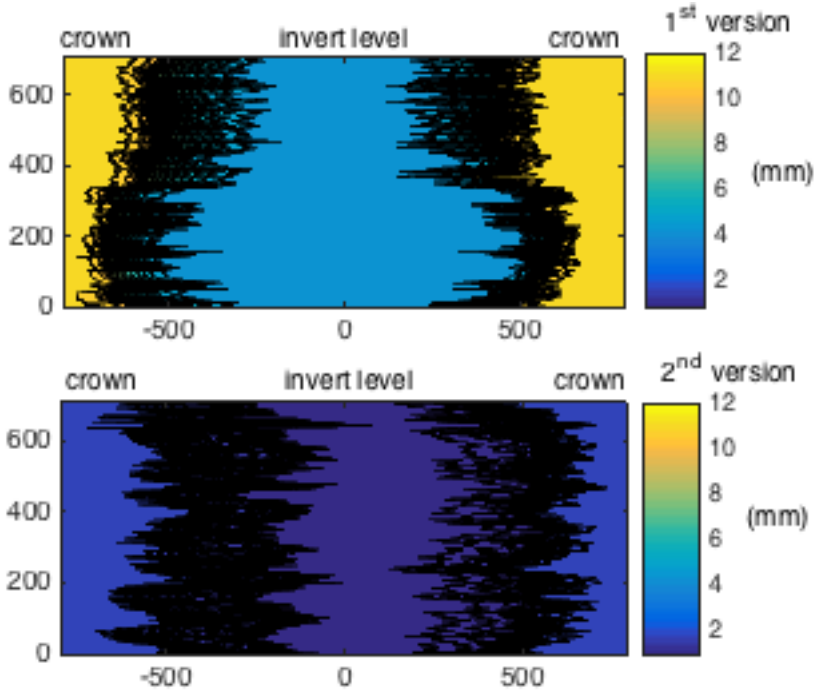

Figure 5. Difference between uncertainties associated to the estimation of the loss of wall thickness (top: old version, bottom: new version).

Some sediments (sand, gravels and various sizes stones) were pasted on a PVC half down-pipe to measure and calculate different roughness with the profiler. Table 2 presents the roughness (K_S) estimated of the scanned sediments (Stanic *et al*, 2015). However, standard uncertainties ($u(K_S)$) are in the same order of magnitude as the wall roughness. The proposed prototype is not enough accurate to estimate the wall roughness with an acceptable confidence interval.

Table 2. Results of the roughness calculations.

Material	Granulometry	K_S mm	$u(K_S)$ mm
Sand	-	1,74	2,01
Gravel	5-8 mm	6,13	2,26
Small stones	22-30 mm	11,25	2,68
Medium stones	30-40 mm	15,62	3,07
Large stones	40-63 mm	17,34	3,66

CONCLUSIONS AND PERSPECTIVES

The potential applications of the improved laser profiling techniques are comprehensive *e.g.* replacement of subjective and inaccurate CCTV or deposit measurements. Collected data on 3D geometry may be used to study pipe-collapsing behaviour and efficiently plan maintenance works.

The new design of the apparatus and the improvements in the protocol applied (camera and laser distance meter calibrations) offers an accuracy up to 5-10 times higher than the previous version. This version is still not accurate enough to be suitable for *in-situ* roughness measurements, which may be used as input data for CFD modelling instead of common, and maybe wrong (especially for an existing sewer), assumptions.

Additionally to a higher accuracy, there are several improvements that can be applied to a potential third version of the prototype. Currently the amount of raw data that is generated during the experiment data acquisition over the 1 m of pipe length is around 4.86 GB: the data flow is too high for an embedded application but this can be significantly reduced. There are still some improvements to be done with the presented hardware to make the data acquisition faster and lighter.

Such a device requires empty pipes to measure deposits and to be able to see defects below the water surface. Future developments will aim at: *i)* increasing the accuracy (standard uncertainty up to 0.1 of 0.2 mm) in order to accurately estimate the roughness; *ii*) improving the design and mathematical methods to process data of such a laser profiler; *iii*) possibilities of use pattern recognitions of pipe defects (to prevent subjectivity in data interpretation as for CCTV) and *iv)* to propose new devices *e.g.* combining techniques and measurement methods to assess submersed parts of the pipe, to identify misconnections and to make inspections easier (without disruption of the sewer service).

ACKNOWLEDGEMENT

The authors would like to acknowledge the funding by (in alphabetical order) ARCADIS, Deltares, Gemeente Almere, Gemeente Breda, Gemeente's-Gravenhage, Gemeentewerken Rotterdam, Gemeente Utrecht, GMB Rioleringstechniek, Grontmij, KWR Watercycle Research Institute, Royal HaskoningDHV, Stichting RIONED, STOWA, Tauw, vandervalk+degroot, Waterboard De Dommel, Waternet and Witteveen+Bos as part of the Urban Drainage Research program. A special word of thank goes to vanderValk+deGroot and Deltares for giving access to their facilities. In addition, this work was also part of the Marie Curie Initial Training Network QUICS project. This project has received funding from the European Union's Seventh Framework Programme for research, technological development and demonstration under grant agreement No. 607000.

REFERENCES

Wirahadikusumah R., Abraham D.M., Iseley T. and Prasanth R.K. (1998). Assessment technologies for sewer system rehabilitation. Automation in Construction, **7**, pp. 259-270.

Kirkham R., Kearney P.D., Rogers K.J. and Mashford J. (2000). PIRAT—a system for quantitative sewer pipe assessment. *The International Journal of Robotics Research*, **19**, pp. 1033-1053.

Dirksen J., Clemens F. H. L. R., Korving H., Cherqui F., Le Gauffre P., Ertl T., Plihal H., Müller K. and Snaterse C. (2013). The consistency of visual sewer inspection data. *Structure and Infrastructure Engineering*, **9**(3), (2013) 214-228.

Clemens F. H. L. R., Stanić N., Van der Schoot W., Langeveld J., Lepot M. (2014). Uncertainties associated with laser profiling of concrete sewer pipes for the quantification of the interior geometry. *Structure and Infrastructure Engineering*, **11**(9), pp.1-22.

Dimetix . (2012). FLS-C10 Technical Reference Manual V5.02, downloaded the 26th of July 2015 here: (http://www.dimetix.com/downloads/Manuals/DLS_FLS_C_TechnicalManual_V502_en.pdf).

Heikkila J. and Silvén O. (1997). A four-step camera calibration procedure with implicit image correction. *Computer Vision and Pattern Recognition*, in Proceedings of: IEEE Computer Society Conference on, pp. 1106-1112.

Stanić N., Clemens F. H. L. R., Lepot M. and Langeveld J.G.. (2015). Estimation of hydraulic roughness of concrete sewer pipes by laser scanning,*J. of Hydr. Eng*. (submitted).